Mechanism of Asphalt Heating with Thermal Oil Based on Biomass Boilers

Dengke Zhao,[a] Shengyong Liu,[a,*] Tengfei Lv,[a] Enhai Liu,[a,b,*] Xianghe Liu,[b] Guojiang Chen,[c] and Xin Huang [b]

Biomass-fired thermal oil heaters are green and efficient heating devices that use heated thermal oil as the heat transfer medium. This study investigated how thermal oil thermophysical properties and heating temperature affect asphalt heating. A physical model incorporating thermal convection and conduction was established, computational fluid dynamics (CFD) simulations using hypothetical single-factor property combinations were conducted to analyze the effects of thermal oil density, specific heat capacity, and thermal conductivity. An independent experimental platform using a biomass thermal oil boiler and real thermal oils was constructed to examine the simulated property effects. Results show that the specific heat capacity and density of thermal oil dominate heat transfer during the early heating stage by altering the internal energy carried by the fluid. In contrast, the extremely low thermal conductivity of asphalt constitutes the primary bottleneck for system heat transfer, limiting the influence of thermal oil thermal conductivity on overall heating performance. Experimental trends support the simulated property effects. Within the tested property ranges, the influence ranking based on experimental temperature differences is: specific heat capacity > density > thermal conductivity. At 1000 s, the corresponding absolute temperature differences between the high- and low-parameter cases are 1.97, 0.91, and 0.2 °C. These findings provided theoretical support and design guidance for the matching of operating conditions and thermal oil selection in biomass-powered indirect heating systems.

DOI: 10.15376/biores.22.1.42-70

Keywords: Biomass heater; Thermal oil; Thermophysical properties; Numerical simulation; Computational Fluid Dynamics

Contact information: a: College of Mechanical & Electrical Engineering, Henan Agricultural University, Zhengzhou 450002, China; b: School of Urban Construction, Changzhou University, Changzhou 213164, China; c: Binhu District Guojiang Enterprise Consulting Service Co., Ltd, Wuxi 214125, China;
** Corresponding authors: liushy@vip.sina.com; liuenhai1018@126.com*

INTRODUCTION

As an eco-friendly and sustainable thermal energy conversion device, biomass boilers are increasingly becoming an important alternative to traditional fossil fuel–fired heating equipment (Zhang *et al*. 2022; Xu *et al*. 2025). Their core advantage lies in the use of renewable biomass resources, such as agricultural and forestry residues, as fuel, which not only substantially reduces net carbon dioxide emissions in line with the "dual carbon" strategic goals but also realizes high-value utilization of waste resources (Mao *et al*. 2022).

Typical biomass heaters convert the chemical energy of biomass into thermal energy *via* gasification or direct combustion. Featuring wide fuel availability, low operating costs, and environmental friendliness, biomass shows broad application prospects in fields requiring stable heat sources, such as district heating, industrial drying, and especially road asphalt production (Ma *et al*. 2020).

Efficient, uniform, and stable heating is critical in road asphalt production. Direct heating of asphalt using flue gas from biomass combustion faces challenges including inaccurate temperature control, local overheating, and low thermal efficiency (Hu *et al*. 2018). Therefore, the introduction of thermal oil as an intermediate heat carrier has become a key technical approach to improving overall system efficiency (Yu *et al*. 2019). The working principle and system flow are shown in Fig. 1a. Biomass fuel is fully combusted in the combustion chamber, generating high-temperature flue gas. This high-temperature flue gas first exchanges heat with the outer wall of the thermal oil tube bundle *via* forced convection, while simultaneously transferring radiative heat to the tube wall through high-temperature thermal radiation. Heat then penetrates the tube wall and is transferred to the flowing thermal oil inside the tubes (Ji *et al*. 2019).

The heated thermal oil is delivered to the asphalt heating unit through a series-parallel pipeline system. In the pipeline, heat is transferred to asphalt through conduction across the tube wall. Meanwhile, the thermal oil flow provides forced convection inside the tubes (Cui 2010). The installed asphalt agitator was not operated in the present experiments. Investigating the heat transfer characteristics and optimal application of thermal oil in this composite heat transfer system is of great engineering significance for improving asphalt heating efficiency and enhancing the practicality and competitiveness of biomass heaters in this field. The principle of biomass thermal oil heater heating asphalt and the biomass thermal oil boiler are shown in Fig. 1a and 1b, respectively.

The material heated in this study is asphalt binder. Heat is transferred from the thermal oil to the asphalt through the walls of the heating tubes. The thermal conductivity of asphalt affects heat conduction within it, while its specific heat capacity determines the sensible heat required for a given mass and temperature rise. These properties differ from those of aggregate-containing asphalt mixtures (Guo *et al*. 2024). At the mixing plant, the heated asphalt binder is mixed with aggregates to produce asphalt mixtures for pavement construction. As described in the Federal Highway Administration's technical brief FHWA-HRT-15-052 (2018), asphalt undergoes oxidative aging during heating in contact with air, which changes its chemical and rheological properties. Oxidation makes the binder stiffer and more brittle and slows stress relaxation, increasing its susceptibility to thermal cracking. Higher temperatures accelerate oxidation, while longer exposure allows aging to progress. Heating should therefore meet the required production temperature while limiting local overheating and the time spent at high temperatures. Commercial thermal oils include mineral-oil-based and synthetic organic fluids. Technical data for Shell Heat Transfer Oil S2 and Eastman Therminol 55 and VP-1 provide examples of their compositions: highly refined mineral oils, synthetic hydrocarbon mixtures, and biphenyl/diphenyl ether mixtures, respectively. These fluids differ in their operating temperature ranges, thermal stability, and viscosity.

The intended application is asphalt tank heating at asphalt mixing plants, with the boiler located within the plant to supply heat. For practical implementation, the boiler location, biomass fuel delivery and storage, and ash collection and removal should be planned around the plant roads and working areas to keep vehicle routes clear.

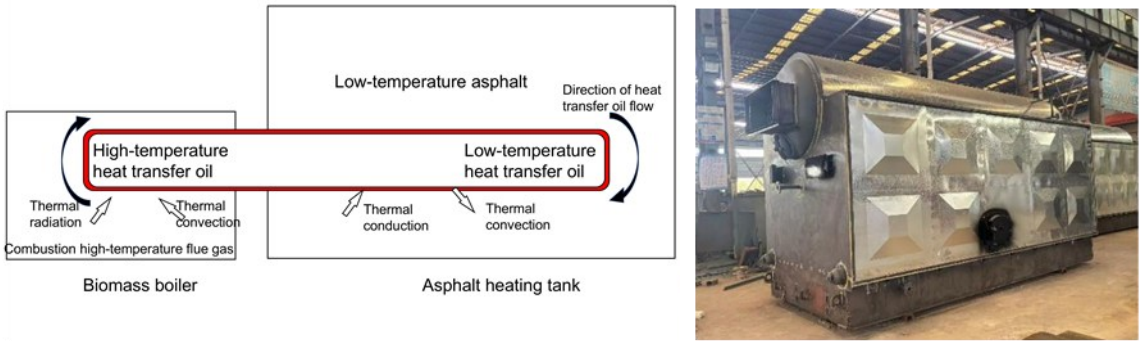


Fig. 1. (a) Schematic of asphalt heating by a biomass thermal oil heater; (b) Biomass thermal oil boiler

To date, numerous scholars have conducted extensive research on biomass boilers and thermal oil heating systems, focusing mainly on biomass combustion characteristics, boiler thermal efficiency evaluation, and fundamental heat transfer performance analysis of thermal oil as a heat transfer medium. Basu (2018) systematically reviewed modeling methods and operational characteristics of biomass combustion and boiler thermal behavior, with emphasis on furnace temperature distribution and energy conversion efficiency. Obernberger and Thek (2004) and Demirbas (2004) conducted in-depth analyses of thermal efficiency and fuel calorific value characteristics of biomass boilers from the perspectives of fuel and system operation. Meanwhile, studies on thermal oil as a heat transfer medium have mostly focused on the effects of thermophysical properties, such as density, specific heat capacity, and thermal conductivity, on convective heat transfer performance, with wide applications in industrial heating and energy system analysis (Laing *et al*. 2011).

Recent studies have addressed thermal-oil heating from the perspectives of system operation, heat-transfer enhancement, and fluid selection. A biomass boiler coupled to a thermal-oil circuit and a recuperative organic Rankine cycle (ORC) was experimentally investigated, focusing on performance under design and off-design conditions (Falbo *et al*. 2025). A numerical comparison of high-temperature thermal-oil flow in straight, helical, and internally torsion-ribbed helical tubes showed that the ribs enhanced heat transfer and improved temperature uniformity (Wu *et al*. 2024). A comparison of three industrial thermal oils in an ORC coupled with thermal energy storage showed that, within the investigated conditions, system configuration and operating conditions were more influential than the choice among the tested oils (Birriel *et al*. 2025). These studies address system-level performance and oil-side heat transfer. The present study examines the individual effects of thermal-oil density, specific heat capacity, and thermal conductivity on the transient heating response of asphalt under common numerical geometry and boundary conditions.

The numerical analysis focuses on the asphalt heater, with thermal oil temperature and velocity prescribed at the inlet of the heating tubes. This study adopted computational fluid dynamics (CFD) numerical simulation and established a three-dimensional simulation model of the biomass-thermal oil asphalt heating system using the ANSYS Fluent platform. A numerical model with geometric structure and boundary conditions is constructed. Through setting hypothetical single-factor thermal oil cases with different specific heat capacity, thermal conductivity, density, and heating temperature, the flow and heat transfer processes in heating pipes are systematically simulated. Through solving

momentum and energy equations, the influences of each parameter on heat transfer rate, area-averaged thermal oil outlet temperature, and volume-averaged asphalt temperature are qualitatively analyzed, revealing the heat transfer enhancement mechanism and energy efficiency restriction under the synergistic effect of thermophysical properties. An experimental platform for asphalt heating using a biomass thermal oil boiler is built to quantitatively analyze the effects of thermal oil properties on heating performance and examine the trends in property effects using real thermal oils. The numerical model and experimental platform are independent; the comparison concerns property effects. Here, inlet refers to the thermal oil inlet of the heating tubes in the asphalt heater.

PHYSICAL MODEL AND EXPERIMENTAL SETUP

Physical Model

In this study, a three-dimensional model of an asphalt heater was established based on the structure of a practical asphalt heater (Yang 2016), as shown in Fig. 2. The asphalt heater mainly consists of the following components: heating tubes, external enhanced heat transfer fins, thermal oil inside the heating tubes, and the outermost asphalt zone. Due to the low thermal conductivity of asphalt, the external heat transfer fins maximize the heat exchange area between the heating tubes and asphalt, thereby improving heating efficiency (Li *et al*. 2019; Peng *et al*. 2022). The tube walls and fins are included as solid domains in the conjugate heat-transfer calculation.

The dimensions of the numerical model are as follows: inner wall size of the heater: 800 mm × 800 mm × 1100 mm; inner diameter of the heating tube: 20 mm; wall thickness: 1 mm. Length of enhanced heat transfer fins: 700 mm; width: 250 mm; thickness: 10 mm; number of fins: 9; tube bending radius: 30 mm. The numerical model is shown in Fig. 2. Thermal oil enters through P1 and P2 and leaves through the corresponding outlets P3 and P4, respectively, as indicated by the arrows in Fig. 2.

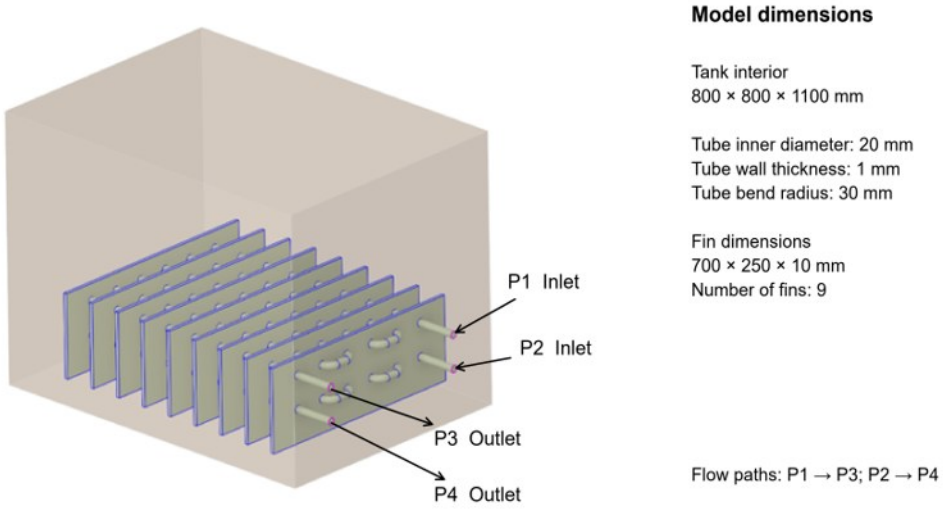


Fig. 2. Physical model

A three-dimensional model is used to retain the bends and fin arrangement in the numerical geometry and to calculate oil temperature variation along the tubes, as well as temperature distributions and buoyancy-driven flow within the asphalt. In a one-dimensional model representing heat transfer only across the tube wall, the spatial arrangement of bends and fins, differences in heat-transfer paths, and transverse temperature variations would require equivalent parameters or simplified relationships. The three-dimensional model allows the effects of thermal oil properties on overall heating performance to be compared under the same geometry and boundary conditions.

Mesh Generation

Figure 3(a) shows the mesh of the asphalt region, while Fig. 3(b) shows the mesh at the outlet cross-section of the heating tube, corresponding to the thermal oil outlet boundary of the numerical model. Fluent Meshing was used for mesh generation, with a maximum element size of 8 mm and a minimum size of 1 mm. A size function was applied for local control. The proximity to the inner walls of fins and heating tubes was set to 3 to ensure at least 3 mesh layers near fins and inner tube walls.

The normal angle for mesh curvature was set to 5° to accurately capture the curvature of the heating tubes. To precisely resolve the flow and thermal boundary layers at fluid–solid interfaces, boundary layer meshing was applied at the interfaces between fluid and solid domains. The first layer thickness of the boundary layer accounted for 0.272 of the first grid thickness; the growth rate was set to 1.2; the number of layers was 3; and the minimum orthogonal quality was 0.35 (Cui 2014; Palanisamy 2024).

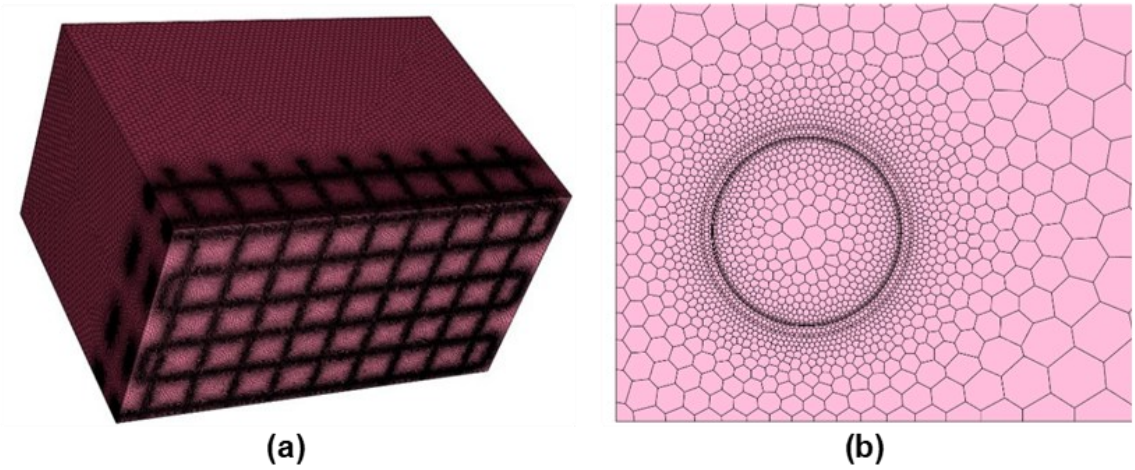


Fig. 3. (a) Asphalt-region mesh; (b) Mesh at the heating-tube outlet cross-section

Governing Equations for Physical Processes

The operation of the asphalt heater mainly involves the flow and heat transfer of thermal oil. Because the dominant heat transfer mechanisms between asphalt and heating tubes and between tubes and thermal oil are conduction and convection, radiative heat transfer is neglected in the heating process. Accordingly, the flow and heat transfer inside the asphalt heater and thermal oil follow three fundamental conservation equations (Chen *et al*. 2017; Qin *et al*. 2021), as given in Eqs. 1-1 to 1-4.

1) Mass Conservation Equation

$$\frac{\partial \rho}{\partial_{\mathrm{t}}} + \nabla \rho U = 0 \qquad (1-1)$$

2) Momentum Conservation Equation

$$\frac{\partial \rho U}{\partial_{\mathrm{t}}} + \nabla \rho U \times U = -\nabla P + \nabla \tau + \rho g \qquad (1-2)$$

$$\tau = \mu(\nabla U + \nabla^{\mathrm{T}} U) \qquad (1-3)$$

3) Energy Conservation Equation

$$\frac{\partial \rho c_{\mathrm{p}} T}{\partial t} + \nabla \rho c_{\mathrm{p}} T U = -\nabla(\lambda \nabla T) \qquad (1-4)$$

where ρ is the fluid density (kg/m^3), $U = (u,v,\omega)$ denotes the velocity components in the x, y, and z directions (m/s), μ is the dynamic viscosity of the fluid (Pa·s), t is time (s), P is pressure (Pa), T denotes temperature (K), λ denotes thermal conductivity (W/m·K), τ denotes shear stress (Pa), g denotes gravitational acceleration taken as 9.81 m/s^2, c_p is the specific heat at constant pressure (J/kg·K), and $\nabla = \frac{\partial}{\partial x}\mathrm{i} + \frac{\partial}{\partial_y} j + \frac{\partial}{\partial z} k$ is the gradient (del or nabla) operator (m^{-1}) (Chen *et al*. 2023). Temperature is expressed in K in the governing equations and numerical solver. Numerical and experimental temperature results are reported in °C, with numerical temperatures converted using T(°C) = T(K) − 273.15. Temperature differences and rates of temperature change retain the same numerical values when converted from K to °C and from K/s to °C/s, respectively.

Inside the heating tubes, heat conduction is the dominant heat transfer mode, and its governing equation is as follows:

$$\nabla \cdot (\lambda \nabla T) + S_{\mathrm{Q}} = 0 \qquad (1-5)$$

where λ is thermal conductivity and SQ is the volumetric heat source, which is zero in non-source regions (Hu *et al*. 2024).

Model Assumptions and Boundary Conditions

To simplify the physical process of asphalt heating by thermal oil, an efficient computational model capable of capturing realistic physical behavior was constructed. Based on the indirect heating system of asphalt by thermal oil, the following physical assumptions and boundary conditions were adopted in this study:

1) Thermal oil is heated in the biomass furnace and is treated as a Newtonian fluid. Density, specific heat capacity, and thermal conductivity are constant within each numerical case and are varied separately between cases for single-factor comparisons. Dynamic viscosity is fixed at 0.001 Pa·s in all numerical cases, with no viscosity–temperature relation applied. In real thermal oils, temperature-dependent viscosity affects the Reynolds number and convective heat transfer. The property effects reported here are obtained from flow and heat-transfer calculations under the specified constant-property conditions.

2) The combustion process of the biomass boiler is not explicitly modeled. Thermal oil temperature and velocity are prescribed at the inlet of the heating tubes in the asphalt heater.

3) Because asphalt, heating tubes, and other components are opaque, internal radiation is neglected, and only heat conduction and convection are computed.

4) The asphalt heater is well insulated externally with negligible heat loss; thus, the outer surface of asphalt is set as an adiabatic wall.

5) The initial temperature inside the heating tubes and asphalt zone is 26.85 °C (300 K in the solver).

6) The flow is unsteady, and the temporal evolution of temperature during heating is investigated.

7) The Boussinesq approximation is used to account for temperature-induced density variations in the buoyancy term, while treating asphalt density as constant in the other terms of the governing equations (Spiegel and Veronis 1960).

8) The Reynolds number of the thermal oil in the heating tubes is calculated as $Re = \rho u D/\mu$. Using the inlet velocity u = 1 m/s, heating-tube inner diameter D = 0.020 m, and dynamic viscosity μ = 0.001 Pa·s from Table 1 gives Re = 10000 to 40000 for densities of 500 to 2000 kg/m^3. The common reference case B gives Re = 20000. With inlet velocity, tube diameter, and viscosity fixed, the Reynolds number varies with the assigned density between cases. These values support treating the thermal oil flow in the heating tubes as turbulent; the standard k-ε model is used to calculate the flow and temperature fields. A laminar model is adopted to capture buoyancy-driven flow in the asphalt zone (Menter and Matyushenko 2025).

9) Gravity acts vertically downward with a magnitude of 9.81 m/s^2.

10) The thermal oil inlet of the heating tubes in the asphalt heater is specified as a velocity inlet with a constant temperature boundary condition; the inlet velocity is fixed at 1 m/s. The inlet temperature varies compared to heat transfer and asphalt temperature rise under different inlet temperature conditions.

The numerical model describes batch heating of a fixed asphalt charge, with thermal oil flowing through the heating tubes. The asphalt has no inlet or outlet mass flow during heating. Mechanical stirring is not applied; buoyancy-driven flow in the asphalt is included through the Boussinesq approximation and the laminar flow model.

Thermophysical properties of materials

Table 1 lists the thermophysical properties of the materials used in the numerical model.

Table 1. Thermophysical Properties of Materials Used in the Model

Region Name	Density (kg/m^3)	Specific Heat J/(kg·K)	Thermal Conductivity W/(m·K)	Viscosity (Pa·s)	Coefficient of Thermal Expansion
Heating tube	8920	386	378	-	-
Thermal pad	8920	386	378	-	-
Asphalt	1100	1450	0.2	0.01426	0.0009
Thermal oil A	500	1000	20	0.001	-
Thermal oil B	1000	1000	20	0.001	-
Thermal oil C	1500	1000	20	0.001	-
Thermal oil D	2000	1000	20	0.001	-
Thermal oil E	1000	500	20	0.001	-
Thermal oil F	1000	1500	20	0.001	-
Thermal oil G	1000	2000	20	0.001	-
Thermal oil H	1000	1000	5	0.001	-
Thermal oil I	1000	1000	10	0.001	-
Thermal oil J	1000	1000	15	0.001	-

The thermal oil properties were assigned as hypothetical combinations for single-factor comparisons. Density was set to 500, 1000, 1500, and 2000 kg/m^3; specific heat capacity to 500, 1000, 1500, and 2000 J/(kg·K); and thermal conductivity to 5, 10, 15, and 20 W/(m·K). Each property varies over four equally spaced levels, with case B as the common reference. Only one property was changed at a time, while the other properties, geometry, and boundary conditions were held constant. These cases were used to compare the effects of individual thermal oil properties on heat transfer and mean temperature rise.

Cases A, B, C, and D have identical specific heat capacity, thermal conductivity, and viscosity, allowing isolation of the effect of thermal oil density on the heating process. Similarly, cases B, E, F, and G have different specific heat capacities to examine the effect of specific heat capacity. Cases B, H, I, and J have distinct thermal conductivities to reveal the influence of thermal conductivity. The lower heating value ranges of common biomass fuels are shown in Table 2.

Table 2 summarizes the lower heating value ranges of common biomass fuels as background for the boiler heat source. Torrefied biomass pellets offer another fuel option. Increased heating values and improved ignition and combustion characteristics were reported for the biopellets examined in a study of torrefaction (Lee *et al*. 2024). For the same heat demand and boiler thermal efficiency, the required fuel mass is inversely proportional to its lower heating value. A fuel with a higher lower heating value therefore reduces the mass of fuel that must be transported to meet that heat demand. Fuel selection should also consider torrefaction processing costs, transport distance, pellet bulk density, and compatibility with the boiler burner.

Table 2. Typical Lower Heating Values (LHV) of Common Biomass Fuels

Biomass Fuel Type	Lower Heating Value ($MJ \cdot kg^{-1}$)	Typical Application/Form	Reference
Wood pellets	16.5 to 18.5	Industrial pellets	Basu 2018; Demirbas 2004
Wood chips	15.0 to 17.0	Boiler-scale combustion	Basu 2018
Rice husk	13.0 to 15.0	Agricultural residue	McKendry 2002
Wheat straw	14.5 to 17.0	Baled / pelletized straw	McKendry 2002; Obernberger 2004
Corn straw	14.0 to 16.0	Field residue	McKendry 2002; Obernberger 2004
Bamboo	18.0 to 19.5	Dense biomass	Demirbas 2004; Liu 2013
Sawdust pellets	17.0 to 18.8	Processed biomass fuel	Basu 2018; Demirbas 2004

Experimental Setup Construction

An experimental platform for asphalt heating using thermal oil was constructed, with a 0.325 m^3 asphalt heating tank as the core component, combined with a thermal oil circulation system and a thermal oil storage tank. Table 3 lists the thermophysical properties of the thermal oils and asphalt used in the experiments. The experimental platform is independent of the numerical geometry. Each experiment used a fixed charge of asphalt in the asphalt heating tank. No asphalt was added or withdrawn during heating and temperature recording, while thermal oil circulated through the heat exchanger. The experiments therefore followed a batch heating process. The agitator was installed but was not operated during these tests. The experimental heat exchanger consists of a serpentine tube without external fins.

Figure 4 shows the main equipment of the experimental platform, including thermal oil storage tank, asphalt heating tank, coiled-tube heat exchanger, flow meter, agitator, and data monitoring and acquisition system. Figure 5 illustrates the thermal oil circulation system and its instrumentation. The biomass boiler supplies heat to the thermal oil, and the circulation pumps drive the oil through the connected piping. In the asphalt heating tank, the oil transfers heat to the asphalt through the wall of the serpentine heat exchanger; the two materials remain separated. The thermal oil storage tank and expansion tank are connected to the circulation system, with the expansion tank accommodating changes in oil volume during heating. Solid lines represent thermal oil piping, whereas dashed lines represent signal connections between the measuring instruments and the control terminal. The flow meters monitor thermal oil flow, and the thermometers monitor temperatures at the indicated locations. The asphalt temperature measurements are described below and located in Fig. 6.

Table 3. Thermophysical Properties of Thermal Oils and Asphalt Used in Experiments

Name	Density ($kg \cdot m^{-3}$)	Specific Heat Capacity ($J \cdot kg\text{-}1 \cdot K^{-1}$)	Thermal Conductivity ($W \cdot m\text{-}1 \cdot K^{-1}$)	Dynamic Viscosity ($kg \cdot m^{-1} \cdot s^{-1}$)
Thermal oil①	890	2800	0.448	0.000043
Thermal oil②	890	3500	0.448	0.000041
Thermal oil③	890	2500	0.448	0.000042
Thermal oil④	930	2800	0.448	0.000044
Thermal oil⑤	800	2800	0.448	0.000043
Thermal oil⑥	890	2800	0.350	0.000043
Thermal oil⑦	890	2800	0.510	0.000043
Asphalt	940	1900	0.33	-

To measure the spatial temperature distribution of asphalt during heating, a multi-level temperature monitoring network was established inside the heating tank. Eighteen armored Pt100 temperature sensors were employed as core detection units. The probe outer diameter was 6 mm, with a measurement range of -50 to 450 ℃. The single-point measurement accuracy reached ± 0.1 ℃, meeting the requirements for long-term stable monitoring of high-temperature fluid media.

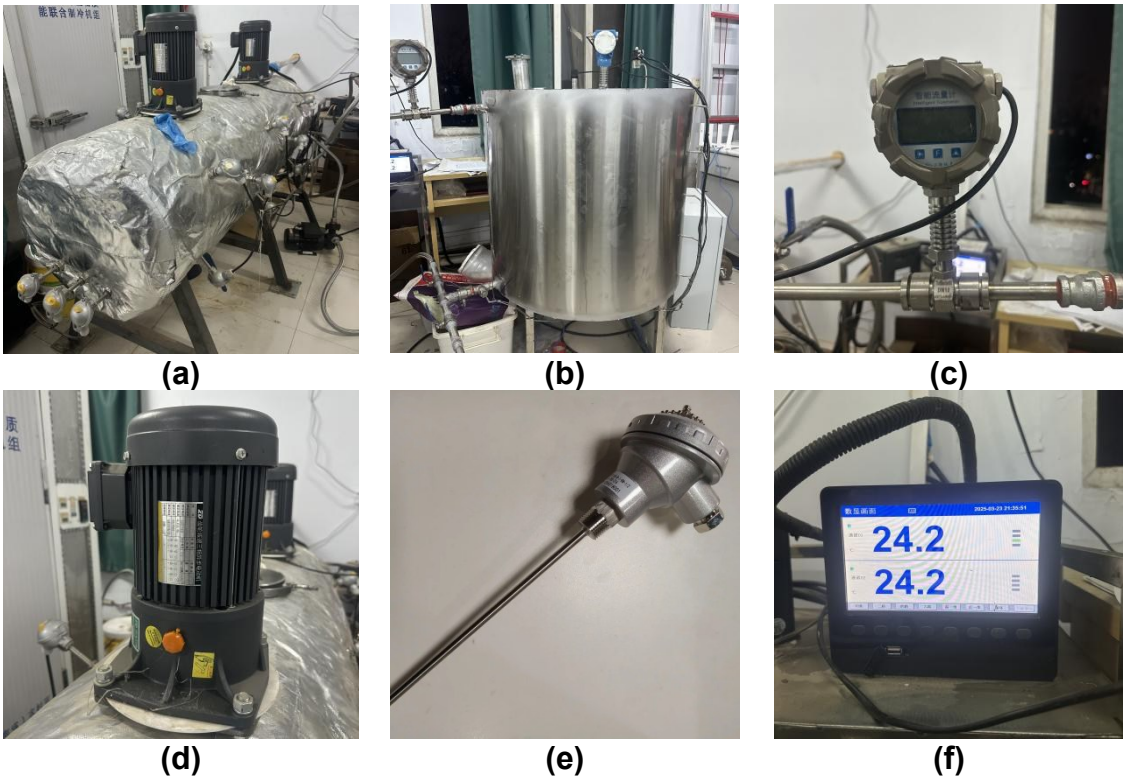


Fig. 4. Main equipment of the experimental platform: (a) asphalt heating tank; (b) thermal oil storage tank; (c) flow meter; (d) agitator; (e) PT100 sensor; (f) temperature display

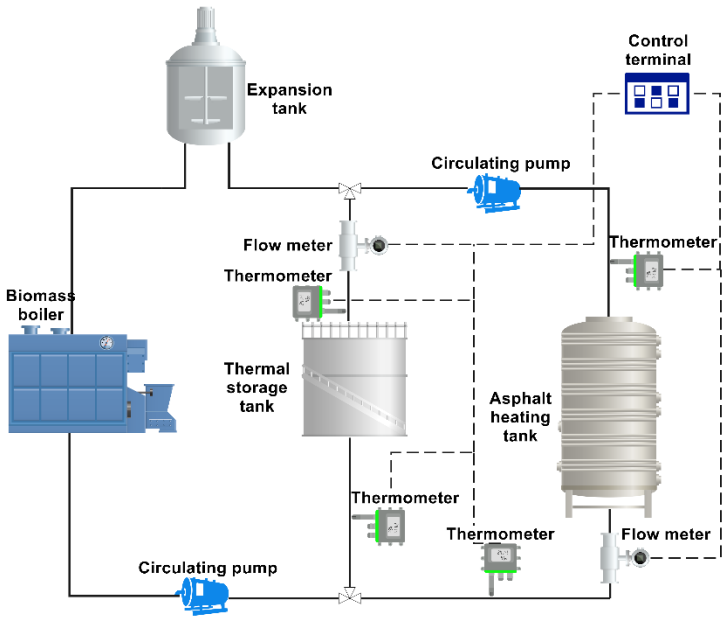


Fig. 5. System flow chart

Spatial positioning used the geometric center of the tank as the origin of the three-dimensional coordinate system, with the tank axial direction defined as the Y-axis. According to the requirement of layered temperature field monitoring, three monitoring planes were divided along the Y-axis from top to bottom, designated as the first to third detection layers. Five temperature sensor nodes were arranged in a circular array on each plane, forming an equally spaced distributed measurement structure.

To enhance the analysis of local heat transfer characteristics, three additional monitoring points were installed at the bends of the serpentine heat exchanger tubes in the tank head region. Meanwhile, one temperature acquisition node was set at both the inlet and outlet pipelines of the thermal oil circulation system, finally forming a distributed temperature monitoring network with 20 measuring points. The three-dimensional schematic of the spatial coordinate parameters of each sensor is shown in Fig. 6.

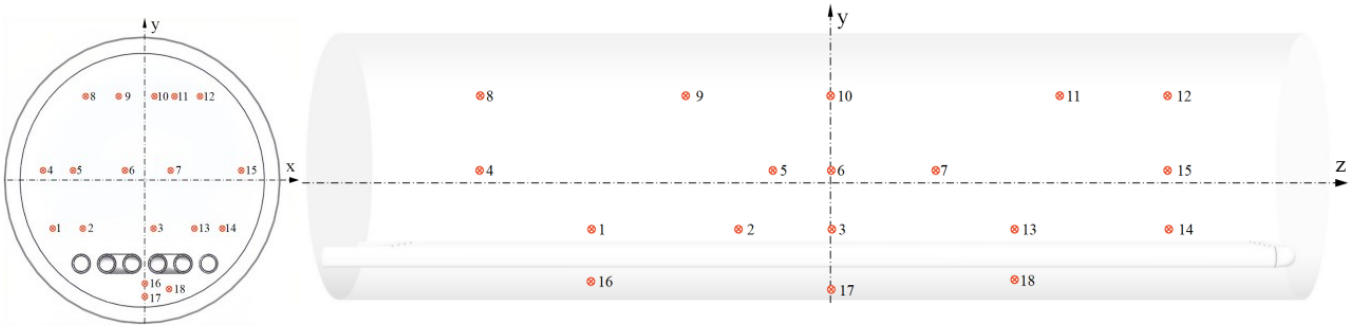


Fig. 6. Measuring points of the temperature field in the asphalt heating tank

Among them, measuring points 19 and 20 are the temperature measuring points at the thermal oil inlet and outlet of the asphalt heating pipeline, respectively, as shown in Fig. 7.



(a) (b)

Fig. 7. Temperature measuring points at the (a) inlet of the asphalt heating tank; (b) outlet of the asphalt heating tank

Excessively high temperatures accelerate the aging of asphalt during processing. Therefore, to maintain stable asphalt performance, the asphalt temperature in heating tanks at mixing plants is usually maintained within 80 to 90 ℃. When production of asphalt concrete is required, asphalt must be heated to approximately 150 ℃ to meet production demands. To better match the actual heating conditions of asphalt mixing plants, an initial asphalt temperature of approximately 80 ℃ was adopted in this experiment.

RESULTS AND DISCUSSION

Analysis of Simulation Results

Effect of thermal oil specific heat capacity on the heating process

Figure 8(a) shows the relationship between heat transfer rate of heating tubes and thermal oils with different specific heat capacities, where the abscissa represents time and the ordinate represents heat transfer rate. It can be seen that at the initial heating stage, high-temperature thermal oil flows into the heating tubes, and thermal oil with higher specific heat capacity presents a higher heat transfer rate. After a certain period of heating, thermal oil with lower specific heat capacity exhibits a relatively higher heat transfer rate. The overall heat transfer rate increases sharply at first and then decreases gradually over time.

This phenomenon occurs because at the initial heating stage, the temperature of thermal oil inside the tubes is low. As high-temperature thermal oil flows in gradually, thermal oil with higher specific heat capacity possesses greater internal energy. Meanwhile, the temperature of asphalt is low, resulting in a large temperature difference between the two media, which leads to a sharp rise in the overall heat transfer rate. The heat transfer rate reaches its maximum when the heating tubes are only filled with high-temperature thermal oil, indicating the largest temperature difference between the high-temperature thermal oil and low-temperature asphalt.

As time elapses, the asphalt temperature increases gradually, and the temperature difference between thermal oil and asphalt diminishes. Consequently, the system heat transfer rate decreases with time and eventually approaches zero (Yao *et al*. 1999).

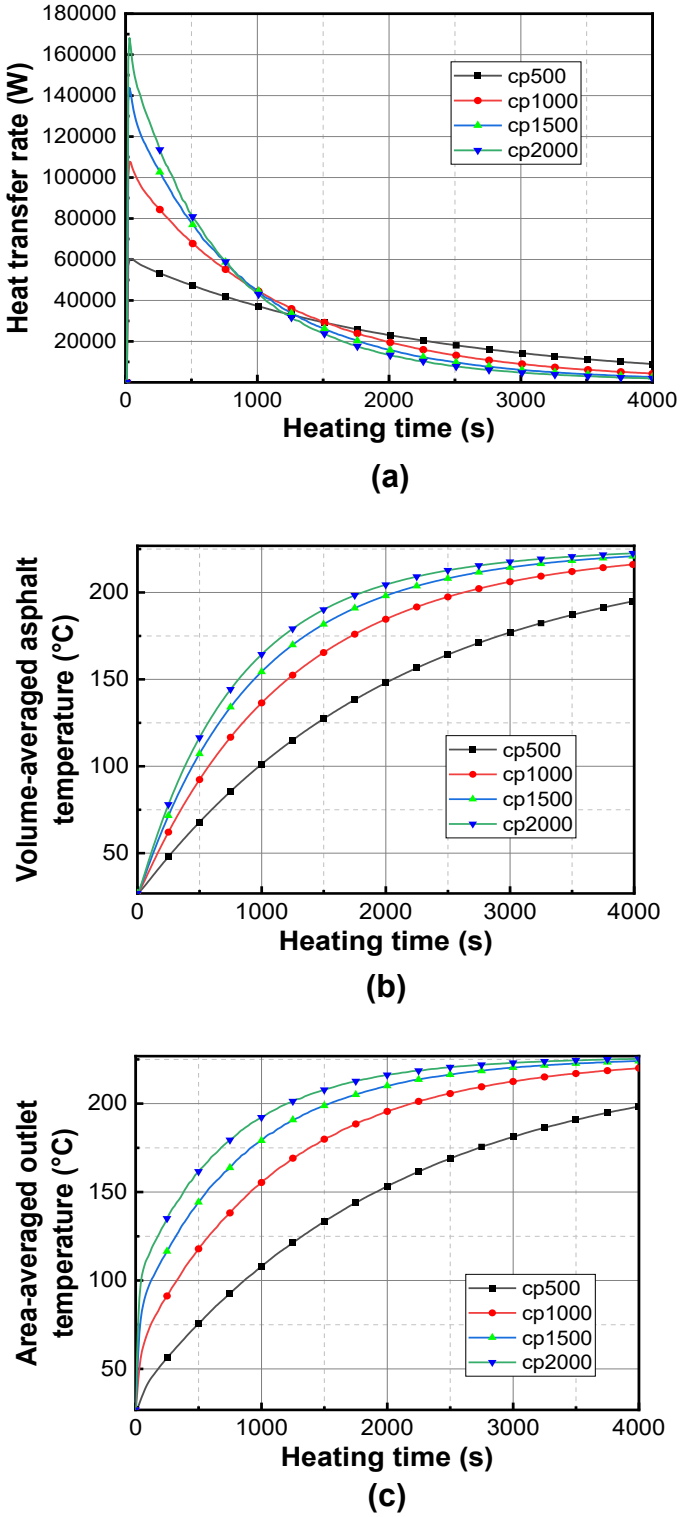


Fig. 8. (a) Effect of thermal oil specific heat capacity on heat transfer rate to asphalt; (b) Effect of thermal oil specific heat capacity on volume-averaged asphalt temperature; (c) Effect of thermal oil specific heat capacity on area-averaged outlet temperature

With continuous heating, asphalt heated by high-specific-heat thermal oil reaches a higher temperature, reducing the temperature difference between the thermal oil and asphalt, which results in a lower heat transfer rate in the second half of heating. In contrast, low-specific-heat thermal oil has smaller internal energy and a faster temperature drop rate, leading to a lower heat transfer rate in the first half. In the second half, the temperature of asphalt heated by low-specific-heat thermal oil remains relatively low, maintaining a considerable temperature difference and thus a higher heat transfer rate (Ma *et al*. 2020).

Figure 8(b) presents the temporal variation of the volume-averaged temperature of asphalt heated by thermal oils with different specific heat capacities, where the abscissa is heating time and the ordinate is the volume-averaged asphalt temperature. It is observed that the heating rate of asphalt is slow at the initial stage. With increasing time, the heating rate first rises and then declines gradually. Meanwhile, using thermal oil with higher specific heat capacity leads to a faster temperature rise of asphalt.

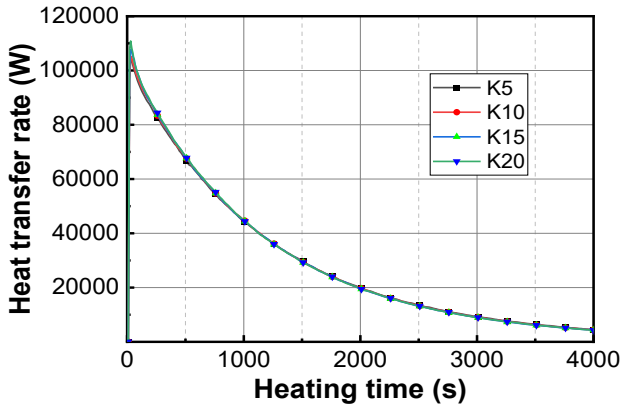
For batch heating, the higher early-stage heat transfer rate contributes to a faster rise in asphalt temperature. As heating proceeds, the decreasing temperature difference between thermal oil and asphalt changes the heat transfer rate. The effect of specific heat capacity is therefore evaluated using both the heat transfer rate and the asphalt temperature over time, so that the early response is considered together with the subsequent heating process.

Figure 8(c) shows the relationship between the area-averaged outlet temperature of thermal oils with different specific heat capacities and time, with time as the abscissa and outlet average temperature as the ordinate. It can be seen that thermal oil with higher specific heat capacity consistently maintains a higher outlet temperature throughout the heating process.

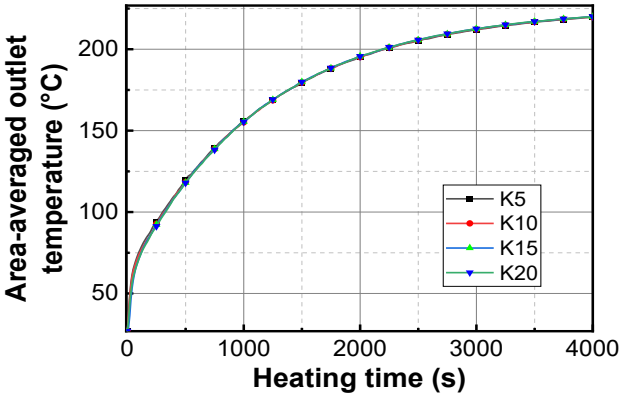
This is because, at the same mass flow rate and temperature, fluids with higher specific heat capacity possess greater internal energy. Given identical heat conduction and dissipation areas in the model, although the heat transfer rate (*i.e.*, internal energy loss rate) differs per unit time, the difference in energy loss is negligible compared with the difference in the inherent internal energy of the fluids. Therefore, high-specific-heat thermal oil always shows a higher outlet temperature.

Effect of thermal oil thermal conductivity on the heating process

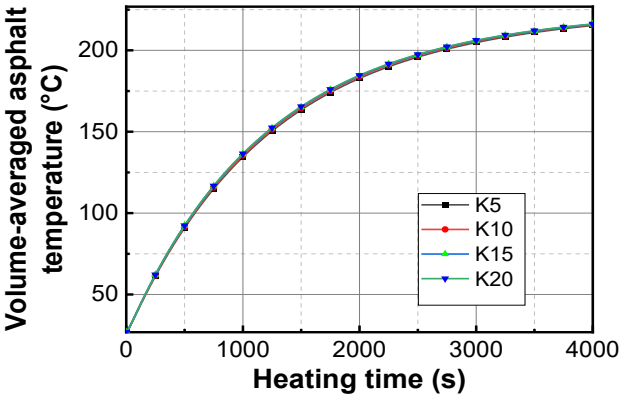
Figure 9(a) shows the relationship between heat transfer rate and time for thermal oils with different thermal conductivities, where the abscissa represents time and the ordinate represents heat transfer rate. It can be seen that the heat transfer rates between asphalt and thermal oils with different thermal conductivities are nearly identical, and the overall heat transfer trend is basically consistent with that of specific heat capacity discussed earlier.


Heat transfer rate (W)
120000
100000
80000
60000
40000
20000
0
1000
2000
3000
4000
Heating time (s)
K5
K10
K15
K20

(a)


Area-averaged outlet temperature (°C)
200
150
100
50
0
1000
2000
3000
4000
Heating time (s)
K5
K10
K15
K20

(b)


Volume-averaged asphalt temperature (°C)
200
150
100
50
0
1000
2000
3000
4000
Heating time (s)
K5
K10
K15
K20

(c)

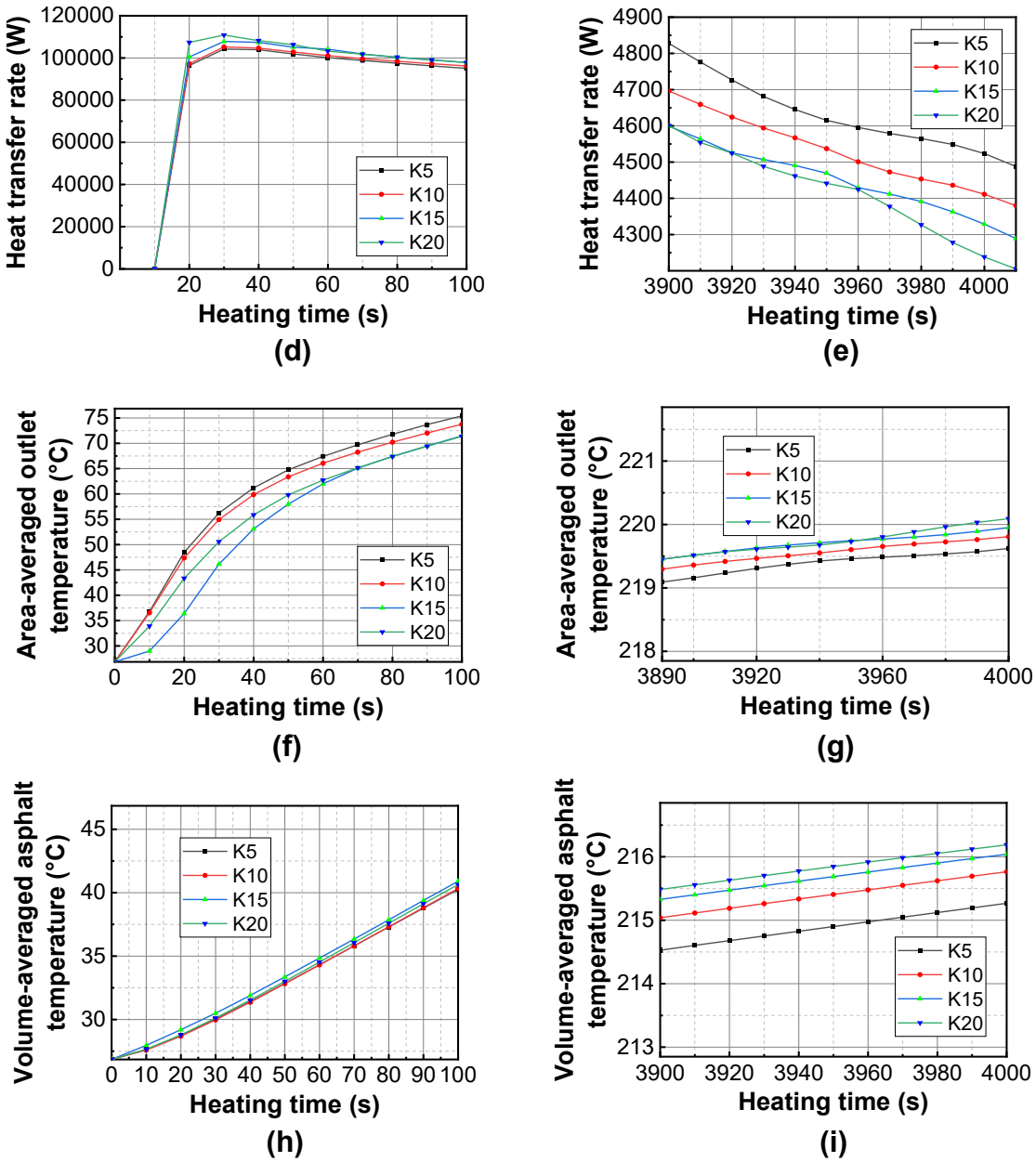


Fig. 9. Effect of thermal oil thermal conductivity on (a) heat transfer rate; (b) area-averaged outlet temperature; (c) volume-averaged asphalt temperature; (d, e) heat transfer rate during the first and last 100 s of heating, respectively; (f, g) area-averaged outlet temperature during the first and last 100 s of heating, respectively; (h, i) volume-averaged asphalt temperature during the first and last 100 s of heating, respectively

Figure 9(b) shows the relationship between the area-averaged outlet temperature of thermal oils with different thermal conductivities and heating time. The abscissa represents time, and the ordinate represents the area-averaged outlet temperature. Overall, the difference in outlet temperature among thermal oils with different thermal conductivities is very small. This is because the inlet velocity and temperature of the model are consistent, and the outlet temperature is directly related to the heat transfer during flow. A larger heat transfer rate leads to a lower outlet temperature, while a smaller heat transfer rate results in a higher outlet temperature.

Figure 9(c) shows the variation of volume-averaged asphalt temperature heated by thermal oils with different thermal conductivities with heating time. The abscissa represents time, and the ordinate represents the volume-averaged asphalt temperature. It can be seen that the thermal conductivity of asphalt limits the heat transfer from thermal oil to asphalt, resulting in almost the same heat transfer rate and thus similar temperature rise rate of asphalt. The thermal conductivity of asphalt is much lower than that of the thermal oil in these numerical cases. This limits heat transfer to the asphalt and accounts for the small differences among the overall responses in Fig. 9(a) to (c). The small differences between the curves are examined using the initial and final 100 s of heating. Figures 9(d) and 9(e) show the corresponding heat-transfer-rate details, respectively.

It can be easily seen that at the initial heating stage, thermal oil with higher thermal conductivity has a higher heat transfer rate due to its stronger heat transfer capability. With the progress of heating, asphalt heated by thermal oil with higher thermal conductivity increase faster. In the late heating stage, asphalt temperature is higher, and the temperature difference between asphalt and thermal oil is smaller. This results in a lower heat transfer rate between thermal oil and asphalt in the late heating stage, and *vice versa*.

Although the low thermal conductivity of asphalt results in a small difference in heat transfer rate, the slight difference in heat transfer still leads to a small difference in outlet temperature. At the beginning of heating, thermal oil with higher thermal conductivity has a higher heat transfer rate and a relatively lower outlet temperature. In the late heating stage, the heat transfer rate decreases, and the outlet temperature of thermal oil with higher thermal conductivity becomes higher instead. The early- and late-stage outlet temperatures are shown in Fig. 9(f) and Fig. 9(g), respectively.

To accurately compare the temperatures of asphalt heated by thermal oils with different thermal conductivities, Fig. 9(h) and Fig. 9(i) show the temperature differences at 100 s after heating starts and 100 s before it ends, respectively. It is obvious that thermal oil with higher thermal conductivity has stronger heat transfer capability (Yao *et al*. 2023).

Effect of thermal oil density on the heating process

Figure 10(a) shows the effect of thermal oils with different densities on heat transfer rate, where the abscissa represents time and the ordinate represents heat transfer rate. It can be seen that the heat transfer rate increases rapidly at the initial stage, then decreases gradually over time, and finally approaches zero. It can also be observed that the heat transfer rate between high-density thermal oil and asphalt is higher in the early heating stage but lower in the middle and late stages.

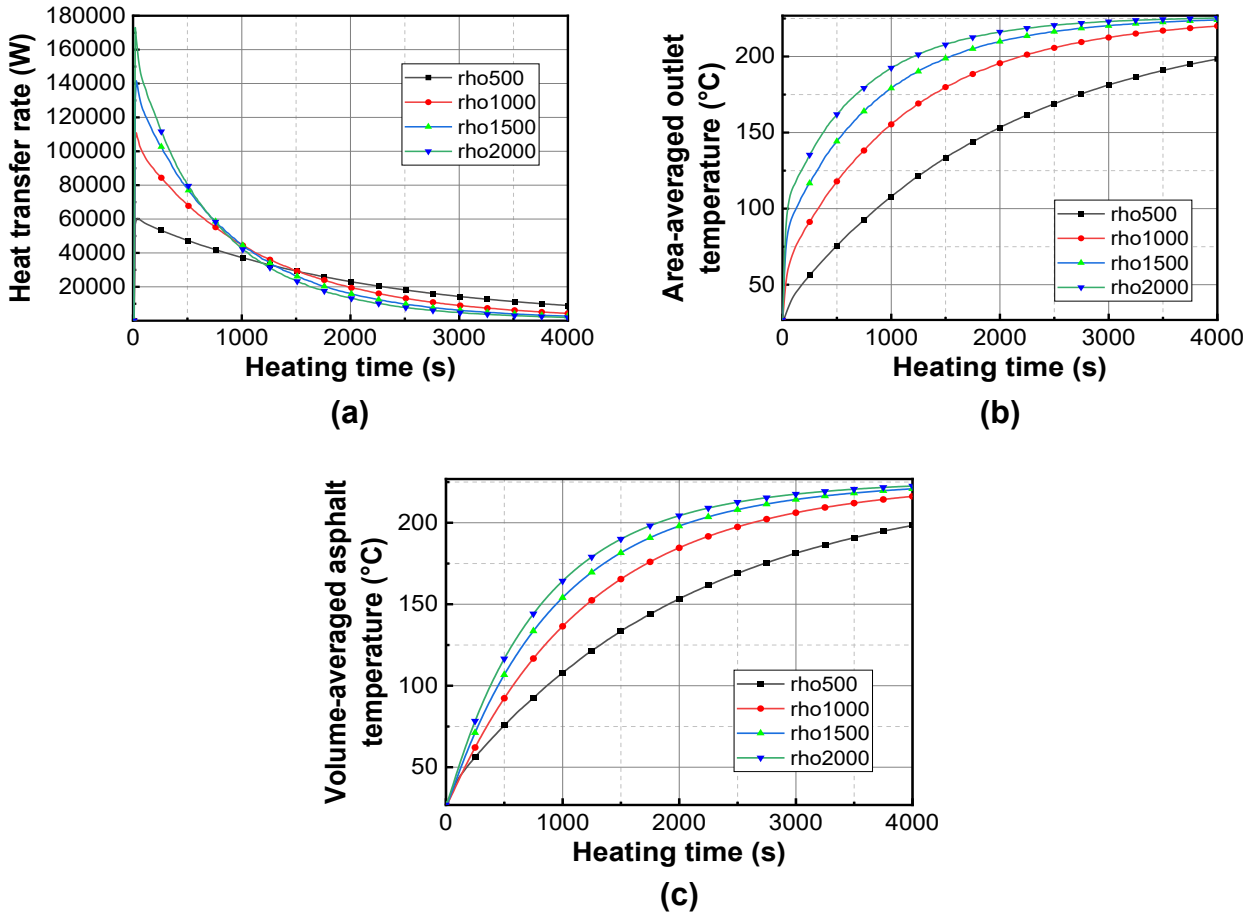


Fig. 10. (a) Effect of thermal oil density on heat transfer rate; (b) Effect of thermal oil density on area-averaged outlet temperature; (c) Effect of thermal oil density on volume-averaged asphalt temperature

The effect of thermal oil density on heat transfer rate is analyzed as follows. The inlet is set to a constant velocity in the model. Therefore, when the density of thermal oil increases, more mass flows into the heating tubes per unit time. Under the same specific heat capacity and temperature, high-density thermal oil has higher internal energy per unit volume.

At the initial heating stage, asphalt temperature is low. High-density thermal oil has higher internal energy and slower energy attenuation, resulting in higher heating efficiency and larger heat transfer rate to asphalt. In the middle and late heating stages, asphalt heated by high-density thermal oil reaches a higher temperature, reducing the temperature difference and thus the heat transfer rate. In contrast, low-density thermal oil has a smaller heat transfer rate in the early stage but a relatively higher rate in the middle and late stages.

Figure 10(b) shows the temporal variation of the area-averaged outlet temperature of thermal oils with different densities, where the abscissa represents time and the ordinate represents outlet temperature. It can be seen that high-density thermal oil has a higher outlet temperature, which increase gradually over time and finally approaches the inlet temperature.

The reason is that with the increase of heating time, asphalt temperature increases gradually, and the temperature difference between asphalt and thermal oil becomes smaller. Therefore, the heat transfer rate decreases gradually, and the temperature drop of thermal

oil becomes smaller, leading to the outlet temperature finally approaching the inlet temperature.

Similarly, high-density thermal oil has higher internal energy per unit volume, while the thermal conductivity and heat transfer area are the same. Therefore, the difference in internal energy per unit volume is much larger than that in heat transfer rate. High-density thermal oil has less energy loss, resulting in a higher outlet temperature.

Figure 10(c) shows the temporal variation of volume-averaged asphalt temperature heated by thermal oils with different densities. The abscissa represents time, and the ordinate represents the volume-averaged asphalt temperature. It can be seen that with the increase of heating time, the temperature rise rate first increase, then decrease gradually, and the maximum temperature approaches the heating temperature. Meanwhile, it can be concluded that asphalt heated by high-density thermal oil reaches the maximum temperature faster. The overall trend of temperature rise rate increasing first and then leveling off is consistent with that of specific heat capacity. When high-density high-temperature thermal oil flows into the heating tubes, its internal energy per unit volume is higher, while the thermal conductivity and cross-sectional area are the same. That is, the difference in heat transfer rate is small compared with the difference in internal energy, leading to less energy attenuation and slower temperature drop of high-density thermal oil. Therefore, asphalt heated by high-density thermal oil reaches the maximum temperature faster. The above results reveal the influence of the laws of thermal oil thermophysical properties on the asphalt heating process. The effect of thermal oil inlet temperature on asphalt heating is examined next.

Effect of thermal oil inlet temperature on the asphalt heating process

In a biomass-thermal oil heating system, the thermal oil inlet temperature is a key operating parameter. This study analyzes its effect on asphalt heating by varying the prescribed inlet temperature.

For the inlet-temperature comparison, four prescribed temperatures of 196.85, 206.85, 216.85, and 226.85 °C (470, 480, 490, and 500 K in the solver, respectively) are used. The inlet velocity is fixed at 1 m/s, and the thermal oil properties are kept unchanged to examine the effect of inlet temperature on heat transfer and asphalt temperature rise.

Figure 11(a) shows the relationship between heat transfer rate and heating time under different thermal oil inlet temperatures. It can be found that the heat transfer rate increases sharply at the beginning of heating and then decreases gradually with time. Meanwhile, the higher the thermal oil inlet temperature, the higher the heat transfer rate, which remains at a relatively high level throughout the heating period.

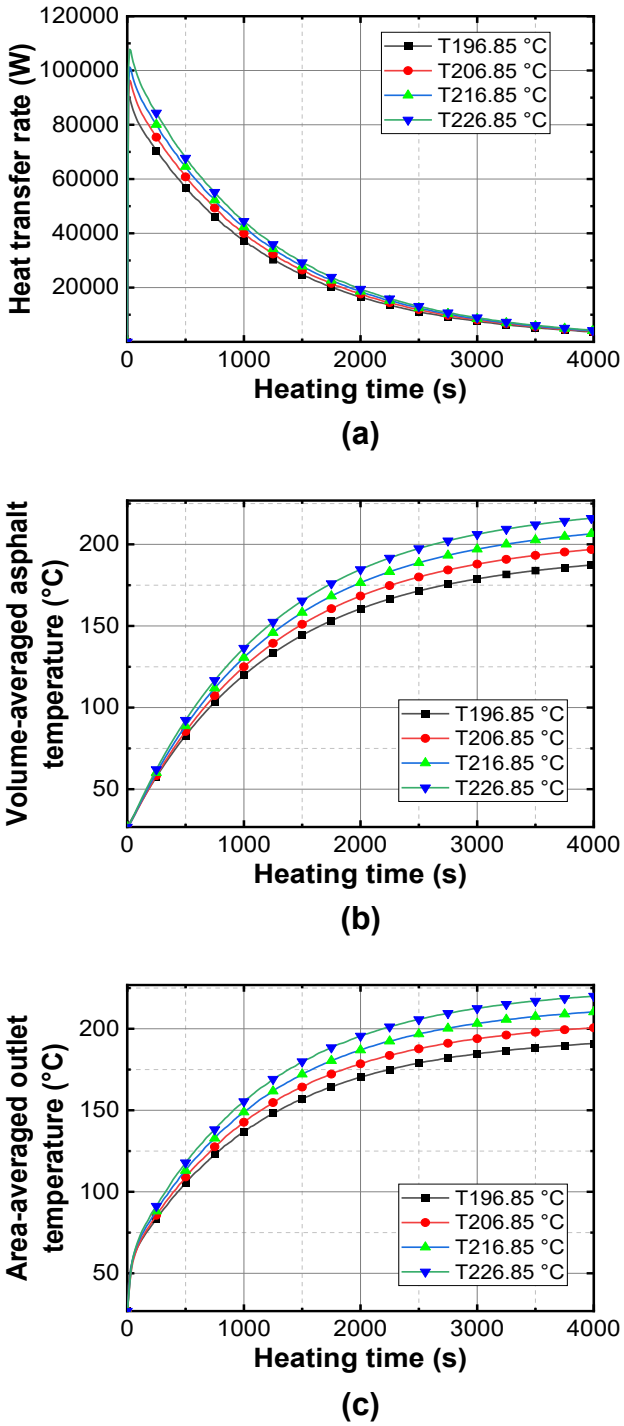


Fig. 11. Effect of thermal oil inlet temperature on (a) heat transfer rate; (b) volume-averaged asphalt temperature; (c) area-averaged outlet temperature

The temporal variation of heat transfer rate has been analyzed in previous sections; the relationship between thermal oil heating temperature and heat transfer rate is explained below. Although the inlet temperatures of thermal oil are different, the initial temperature of asphalt is uniformly 26.85 °C. Therefore, the higher the thermal oil inlet temperature, the larger the temperature difference between thermal oil and asphalt. Correspondingly, higher temperature differences exist between asphalt and heating tubes and between

thermal oil and heating tubes. This enhances convective and conductive heat transfer between thermal oil and heating tubes. As a result, the higher the thermal oil inlet temperature, the greater the heat transfer rate between thermal oil and asphalt.

Figure 11(b) shows the temporal variation of the volume-averaged asphalt temperature during heating by thermal oils with different inlet temperatures. It can be seen that the asphalt temperature increases continuously with heating time. Meanwhile, a higher thermal oil inlet temperature increases the heat transfer rate between thermal oil and asphalt. Consequently, the volume-averaged temperature of asphalt heated by higher-temperature thermal oil is also higher. In addition, the asphalt temperature gradually approaches the thermal oil inlet temperature with time.

Figure 11(c) shows the relationship between the area-averaged outlet temperature of thermal oil and time. It can be observed that the thermal oil outlet temperature increases gradually with heating time and finally approaches the inlet temperature.

During heating, as asphalt is heated, the heat transfer rate between asphalt and thermal oil decreases gradually. The internal energy consumption of thermal oil diminishes, leading to a decreasing temperature difference between the inlet and outlet. This is reflected in the gradual increase of the thermal oil outlet temperature toward the inlet temperature. When the inlet thermal oil temperature is higher, it possesses greater internal energy, a higher heat transfer rate, and a higher outlet temperature.

Analysis of experimental data

It can be seen from Fig. 12 that the volume-averaged asphalt temperature under different thermal oil specific heat capacities rises rapidly at first, then slows down, and finally stabilizes with increasing time. Meanwhile, the temperature derivative curve shows a typical exponential decay characteristic: high initially, decreasing gradually, and approaching zero. This indicates that the system heat transfer rate weakens continuously over time.

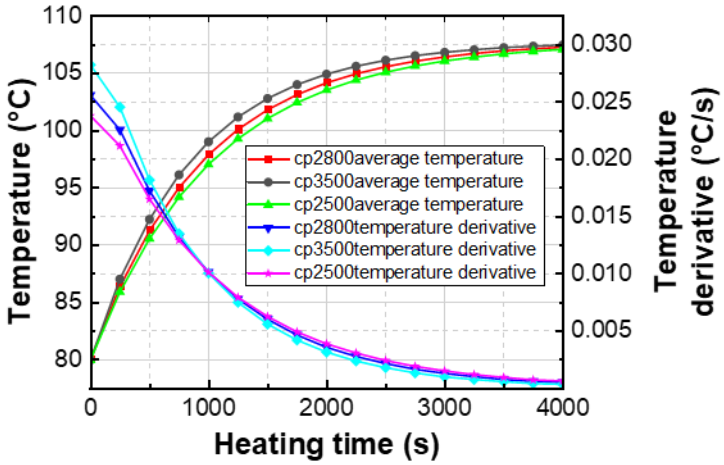


Fig. 12. Effect of thermal oil specific heat capacity on asphalt heating temperature

At 1000 s, increasing the specific heat capacity from 2500 to 3500 J/(kg·K) raises the reported mean asphalt temperature from 97.07 to 99.04 °C, a difference of 1.97 °C. In the initial heating stage (0 to 1000 s), the curves diverge rapidly, and the temperature derivative corresponding to high-specific-heat thermal oil (cp3500) is considerably higher than those of other cases. This indicates its stronger instantaneous heat transfer capability.

This is because thermal oil with a larger specific heat capacity has a higher heat capacity flow rate and slower temperature attenuation during flow. It can maintain a relatively high temperature for a long time, thereby increasing the temperature difference with asphalt. With the progress of heating, the asphalt temperature increases gradually, and the temperature derivatives of all cases decrease continuously. In the middle and late heating stages (beyond 1500 s), the temperature derivative corresponding to low-specific-heat thermal oil (cp2500) becomes higher instead. This trend is consistent with the simulated change in heat transfer rate presented above.

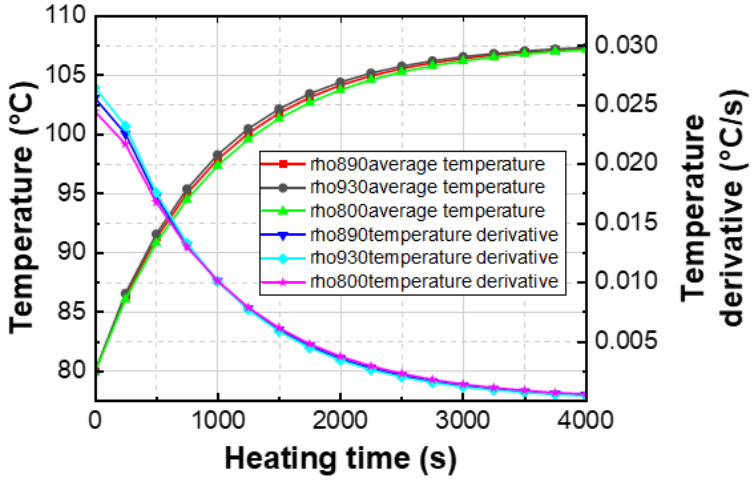


Fig. 13. Effect of thermal oil density on asphalt heating temperature

It can be seen from Fig. 13 that the effect of thermal oil density on asphalt heating is similar to that of specific heat capacity, but the overall difference is considerably smaller and remains stable with time. At 1000 s, increasing the thermal oil density from 800 to 930 kg/m^3 raises the reported mean asphalt temperature by 0.91 °C.

The temperature derivative curves differ greatly in the initial stage (0 to 1000 s) and basically coincide in the later stage. The effect of density on heat transfer is mainly reflected in changing the system heat capacity flow rate by affecting the mass flow rate of thermal oil. When the thermal oil density increases, the mass flow rate rises under the same volumetric flow rate. The heat carried per unit time increases, enhancing the temperature rise of asphalt. Within the tested ranges, the temperature difference for the density group is smaller than that for the specific heat capacity group; normalized sensitivity is compared in Table 4.

It can be seen from Fig. 14 that the volume-averaged asphalt temperature curves almost completely overlap under different thermal conductivities, and the temperature derivative curves are also basically consistent. This indicates that the effect of thermal conductivity on system performance is limited. At 1000 s, the reported mean asphalt temperatures for 0.350 and 0.510 W/(m·K) are 98.01 and 97.81 °C, respectively, differing by only 0.20 °C. The reason is that the main heat exchange process in this study is fluid convection, and the thermal conductivity of thermal oil only affects the local heat transfer resistance. The overall heat exchange process is mainly controlled by temperature difference and heat capacity flow rate. Therefore, thermal conductivity only slightly affects the local initial heat transfer rate and has no pronounced effect on the overall temperature rise and final temperature.

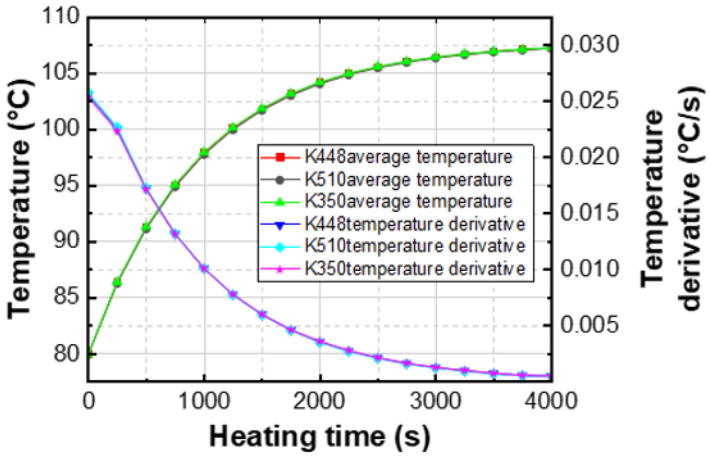


Fig. 14. Effect of thermal oil thermal conductivity on asphalt heating temperature

In summary, the influences of different thermal oil thermophysical properties on asphalt heating efficiency differ considerably. At 1000 s, the absolute temperature difference between the high- and low-parameter cases is largest for specific heat capacity (1.97 °C), followed by density (0.91 °C) and thermal conductivity (0.20 °C). This ordering refers to the tested parameter ranges. This indicates that the system heat transfer process is mainly controlled by the heat capacity flow rate of thermal oil, while thermal conductivity plays a limited role in the overall temperature rise.

To account for the different parameter ranges, the normalized finite-interval sensitivity was calculated using Eq. 1-6,

$$S = \frac{Y_{\text{high}} - Y_{\text{low}}}{Y_{\text{ref}}} \cdot \frac{p_{\text{ref}}}{p_{\text{high}} - p_{\text{low}}} \qquad (1-6)$$

where Y is the mean asphalt temperature rise above the initial temperature and p is the thermophysical property. The subscripts high and low denote cases with the higher and lower values of the property, respectively, and ref denotes the reference case. The numerical reference is case B in Table 1 (initial temperature 26.85 °C); the experimental reference is oil ① in Table 3 (initial temperature 80 °C).

Table 4 presents the temperature differences and normalized sensitivities at 1000 s; their absolute values are used to compare the strength of the property effects. Both comparisons show that specific heat capacity and density have greater effects on asphalt temperature rise than thermal conductivity in both the simulations and experiments.

Table 4. Temperature Differences and Normalized Sensitivity at 1000 s

Study	Property	Range	ΔT (°C)	S
Numerical	Specific heat	500 to 2000	63.19	0.3844
Numerical	Density	500 to 2000	56.35	0.3428
Numerical	Conductivity	5 to 20	2.01	0.0245
Experimental	Specific heat	2500 to 3500	1.97	0.3479
Experimental	Density	800 to 930	0.91	0.3080
Experimental	Conductivity	0.350 to 0.510	−0.20	−0.0313

Note: Property ranges use J/(kg·K), kg/m^3, and W/(m·K), respectively. $\Delta T = T_{high} - T_{low}$. The numerical and experimental reference temperature rises are 109.59 and 17.91 °C, respectively.

To investigate the effect of thermal oil inlet temperature on asphalt heating performance, thermal oil ① in Table 3 was used in this study, and three different thermal oil inlet temperatures were set: 160, 170, and 180 ℃, with an inlet velocity of 2 m/s. The temperature curves of measuring points under the three inlet temperatures are shown in Fig. 15(a to c). Figure 15(a) shows the temperature curve at an inlet temperature of 160 ℃; Fig. 15(b) at 170 ℃; and Fig. 15(c) at 180 ℃.

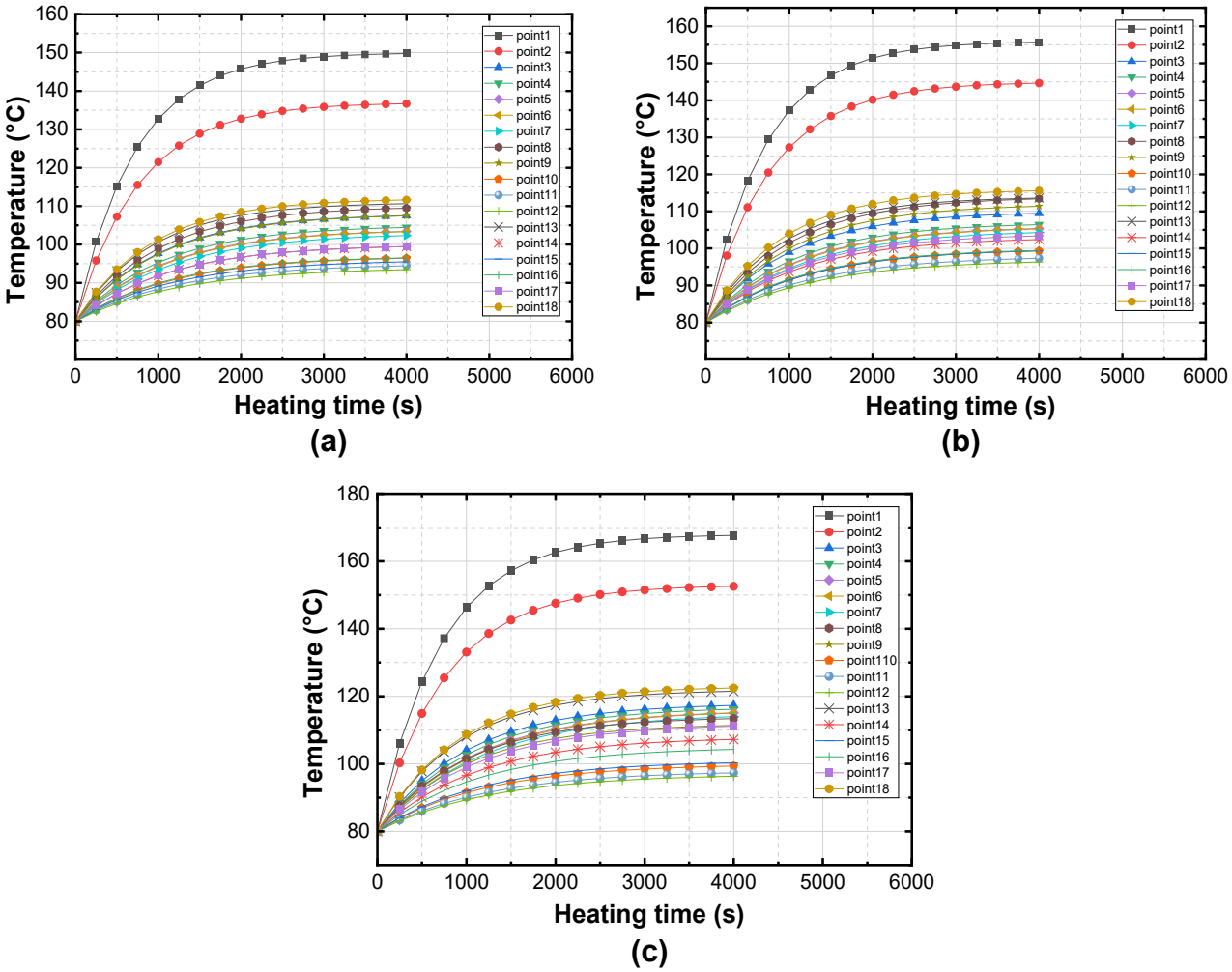


Fig. 15. Temperature of asphalt measuring points at thermal oil inlet temperatures of (a) 160 °C; (b) 170 °C; (c) 180 °C

Comparison of the temperature curves of each measuring point shows that the temperature of Point 1 closest to the inlet increases first, with a heating trend of fast first and then slow. Because the heat exchange between thermal oil and asphalt is realized through convection, the intensity of convection depends on fluid properties and temperature difference. At the initial moment, the asphalt temperature is 80 ℃, while the thermal oil temperature in the heat exchange pipeline is 160 ℃. The temperature difference between them is the maximum in the heat exchange process, and the heat exchange is intense at this time.

As heat exchange proceeds, the asphalt temperature rises gradually, while the thermal oil inlet temperature remains constant at 160 ℃. The temperature difference

between the two media decreases progressively, leading to a gradual slowdown in the heating rate at each measuring point. Measuring Point 12 is the farthest from the thermal oil heat exchange tube, so its temperature remains the lowest among all measuring points, yet its heating trend remains consistent with the others.

Longitudinal comparison of temperature curves under different inlet temperatures reveals that the temperature at each measuring point increases continuously with the increase of thermal oil inlet temperature. Taking Measuring Point 1 as an example, when the thermal oil inlet temperature increases from 160 ℃ to 180 ℃, the temperature at Measuring Point 1 at 4000 s increases from 149.74 to 167.67 °C, a difference of 17.93 °C.

Similarly, for Measuring Point 12, increasing the thermal oil inlet temperature from 160 ℃ to 180 ℃ raises its temperature at 4000 s from 93.43 to 96.31 °C, a difference of 2.88 °C.

Notably, as the thermal oil inlet temperature increases, temperatures at all other measuring points increase to varying degrees. However, this effect is more pronounced for measuring points near the thermal oil heat exchange tube and weaker for those far away.

The experiments were conducted with the asphalt agitator switched off, and temperatures were recorded at different locations over time.

The 0 to 1000 s interval (approximately 16.7 min) is used to compare early heating responses, and the reported comparisons also include 4000 s (approximately 66.7 min). These times provide reference points for comparing the heating responses under the conditions of this study. During asphalt heating at a mixing plant, the time required for the asphalt to reach the target temperature depends on the amount of asphalt, initial and target temperatures, heat-transfer area, and operating conditions.

The results of this study can guide the selection of thermal oils for asphalt mixing plants. Density and specific heat capacity should be evaluated at the intended operating temperatures. Within the conditions examined here, thermal conductivity has a relatively small effect on the heating response; its contribution should therefore be assessed together with the effects of the other properties. Eastman's Therminol fluid selection guidance also identifies operating temperature range, thermal stability, and viscosity as considerations in selecting a thermal oil.

For the same asphalt mass and initial and target temperatures, the sensible heat required by the asphalt is essentially unchanged. The energy implications of differences in heating performance depend on the time required to reach the target temperature, heat losses from the tank and piping, and circulation electricity use. At the same average heat-loss rate, a shorter heating duration reduces cumulative heat loss; at the same pump power, it also reduces circulation electricity use. For cold starts, the heat required to warm the thermal oil and equipment must also be included in the energy balance.

For an illustrative conversion, assuming a biomass lower heating value of 17 MJ/kg and a boiler thermal efficiency of 70%, each 100 MJ reduction in heat supplied by the boiler to the system is expected to reduce biomass consumption by approximately 8.4 kg [100/(17 × 0.70)]. Here, 100 MJ is the reference heat reduction used for the conversion. The corresponding fuel-cost reduction is obtained by multiplying this mass by the fuel purchase price per kilogram. For the same asphalt throughput and heating target, economic comparisons should include fuel costs, circulation electricity costs, and average annual oil purchase and replacement costs calculated over the service life. The allowable operating temperature determines suitability for the heating duty, thermal stability affects replacement requirements, and viscosity affects flow resistance and pumping demand.

Thermal oil selection should therefore consider both heating performance and long-term operating costs.

The comparison shows consistency between the numerical and experimental trends in the effects of the main thermophysical properties, providing experimental support for the applicability of the simulated trends under the tested conditions with real thermal oils.

CONCLUSIONS

1. Increasing the thermal oil inlet temperature from 160 °C to 180 °C raises the arithmetic mean temperature of the 18 experimental measuring points at 4000 s from 106.76 to 115.69 °C, a difference of 8.93 °C. As the thermal oil inlet temperature increases, the heat transfer driving force between the thermal oil and asphalt becomes stronger, resulting in a faster asphalt heating rate and a higher final temperature.
2. During asphalt heating by thermal oil, the specific heat capacity of thermal oil exerts a pronounced effect on the temperature rise of asphalt. Thermal oil with higher specific heat capacity can carry more internal energy under the same conditions, thereby providing a higher heat transfer rate in the early heating stage and substantially accelerating the temperature rise of asphalt. At 1000 s, increasing the specific heat capacity from 2500 to 3500 J/(kg·K) raises the reported mean asphalt temperature by 1.97 °C.
3. Increasing the thermal oil density from 800 kg/m³ to 930 kg/m³ raises the reported mean asphalt temperature at 1000 s by 0.91 °C. Thermal oil with higher density contains more thermal energy per unit volume under the same operating conditions, resulting in a faster asphalt heating rate, particularly during the early stage of heating.
4. At 1000 s, the absolute difference in reported mean asphalt temperature between thermal conductivities of 0.35 and 0.51 W/(m·K) is only 0.2 °C. Because the thermal conductivity of asphalt is much lower than that of thermal oil, the thermal resistance on the asphalt side dominates the heat transfer process. Consequently, the influence of thermal oil thermal conductivity on asphalt heating performance is relatively limited.
5. The results of this study provides a systematic theoretical basis for the selection of thermal oil properties and the matching of heat source conditions in biomass–thermal oil heating systems, and have direct guiding significance for the engineering design and operational optimization of biomass thermal oil boilers.

ACKNOWLEDGEMENTS

This work was supported by Changzhou University Science and Technology Cooperation Project (20250718) and the Jiangsu Province Higher Education Reform Research Project (2025JGYB013)of China.

REFERENCES CITED

Basu, P. (2018). *Biomass Gasification, Pyrolysis and Torrefaction: Practical Design and Theory*, 3rd ed., Academic Press, Cambridge, MA, USA. https://doi.org/10.1016/C2016-0-04056-1

Birriel, A., Romero, J., Saavedra, N., Quinteros-Lama, H., and González, J. (2025). "Thermal and exergetic performance assessment of an ORC coupled with thermal energy storage using thermal oils for low-grade heat recovery," *Applied Sciences* 15(11), article 6153. https://doi.org/10.3390/app15116153

Chen, J. J., Wu, J. J., Ji, X. Y., Lu, X. H., and Wang, C. S. (2017). "Mechanism of waste-heat recovery from slurry by scraped-surface heat exchanger," *Applied Energy* 207, 146-155. https://doi.org/10.1016/j.apenergy.2017.05.111

Chen, M. M., and Xue, Y. B. (2023). "Evolution of Taylor vortex in annular gap flow and its velocity distribution characteristics," *Chinese Quarterly of Mechanics* 44(2), 343-352. https://doi.org/10.15959/j.cnki.0254-0053.2023.02.009

Cui, G. Z. (2010). "Application of heat transfer oil heating system in production of asphalt mixing station," *Northern Communications* 11, 63-65. https://doi.org/10.15996/j.cnki.bfjt.2010.11.002

Cui, L. (2014). "Mesh generation for complex models based on ANSYS FLUENT Meshing," *CAD/CAM and Manufacturing Informatization* 4, 56-58. https://doi.org/10.3969/j.issn.1671-8186.2014.04.040

Demirbas, A. (2004). "Combustion characteristics of different biomass fuels," *Progress in Energy and Combustion Science* 30(2), 219-230. https://doi.org/10.1016/j.pecs.2003.10.004

Falbo, L., Algieri, A., Morrone, P., and Perrone, D. (2025). "Experimental investigation into the energy performance of a biomass recuperative organic Rankine cycle (ORC) for micro-scale applications in design and off-design conditions," *Energies* 18(12), article 3201. https://doi.org/10.3390/en18123201

Guo, M., Yao, X., Fu, Y., and Du, X. (2024). "Characterization of thermophysical parameters of asphalt composites and proposal of computing method of thermal conductivity," *Thermal Science and Engineering Progress* 49, article 102456. https://doi.org/10.1016/j.tsep.2024.102456

Hu, E. F., Zhao, L. X., Wu, J., Meng, H. B., Yao, Z. L., Cong, H. B., and Wu, Y. N. (2018). "Research advance on influence factors and technologies of biomass pyrolysis," *Transactions of the Chinese Society of Agricultural Engineering* 34(14), 212-220. https://doi.org/10.11975/j.issn.1002-6819.2018.14.027

Hu, R., Lv, X., Li, J., Ali, S., and Qi, J. (2024). "The effect of physical property parameters of the insulation material inside the heat shield on the growth of Czochralski silicon crystal," *Silicon* 16(4), 1559-1567. https://doi.org/10.1007/s12633-023-02778-9

Ji, W. X., Zeng, M., Cong, H. B., Yao, Z. L., Meng, H. B., and Zhao, L. X. (2019). "Research status and prospects of biomass pyrolysis reactor," *Biomass Chemical Engineering* 53(3), 46-58. https://doi.org/10.3969/j.issn.1673-5854.2019.03.007

Laing, D., Bahl, C., Bauer, T., Lehmann, D., and Steinmann, W. D. (2011). "Thermal energy storage for direct steam generation," *Solar Energy* 85(4), 627-633. https://doi.org/10.1016/j.solener.2010.08.015

Lee, T.-G., Kim, C.-H., Park, H.-H., Park, J.-H., Park, M.-S., and Lee, J.-S. (2024). "Quality enhancement of torrefied biopellets prepared by unused forest biomass and

wood chip residues in pulp mills," *Applied Sciences* 14(20), article 9398. https://doi.org/10.3390/app14209398

Li, N. S., Tang, Z. C., Wu, J. Y., Zhang, J. L., Xie, A. Z., and Chen, G. S. (2019). "An experimental research of heat transfer of finned-coil phase change heat storage unit," *Journal of Guangdong University of Technology* 36(2), 91-96. https://doi.org/10.12052/gdutxb.180017

Liu, Z. J., Liu, X. E., Fei, B. H., Jiang, Z. H., Cai, Z. Y., and Yu, Y. (2013). "The properties of pellets from mixing bamboo and rice straw," *Renewable Energy* 55, 1-5. https://doi.org/10.1016/j.renene.2012.12.014

Ma, K. R., Zhang, Q. W., Li, S. Q., Hou, N. N., and Feng, L. Y. (2020). "CFD based simulation of heating process by heat conduction oil in oil storage tank," *Journal of Hebei University of Water Resources and Electric Engineering* 30(3), 32-36, +47. https://doi.org/10.16046/j.cnki.issn2096-5680.2020.03.006

Ma, X. Y., Liu, T. T., Cui, S. P., Wang, Y. L., Guo, H. X., and Qin, N. N. (2020). "Research progress on preparation and resource utilization of biomass materials," *Journal of Beijing University of Technology* 46(10), 1204-1212. https://doi.org/10.11936/bjutxb2020050008

Mao, J. X., Guo, H. N., and Wu, Y. X. (2022). "Road to low-carbon transformation of coal power in China: A review of biomass co-firing policies and technologies for coal power abroad and its inspiration on biomass utilization," *Clean Coal Technology* 28(3), 1-11. https://doi.org/10.13226/j.issn.1006-6772.cc22021701

McKendry, P. (2002). "Energy production from biomass (Part 1): Overview of biomass," *Bioresource Technol.* 83(1), 37-46. https://doi.org/10.1016/S0960-8524(01)00118-3

Menter, F. R., and Matyushenko, A. (2025). "Generalized k-ω (GEKO) two-equation turbulence model," *AIAA Journal* 63(11), 4590-4606. https://doi.org/10.2514/1.J065393

Obernberger, I., and Thek, G. (2004). "Physical characterisation and chemical composition of densified biomass fuels with regard to their combustion behaviour," *Biomass and Bioenergy* 27(6), 653-669. https://doi.org/10.1016/j.biombioe.2003.07.006

Palanisamy, V. (2024). "Automotive HVAC performance study using parametric DoE approach for geometric variation with mesh-morphing method in ANSYS fluent (SAE Technical Paper 2024-28-0008)," in: *International Automotive CAE Conference – Road to Virtual World*, Gurugram, India. https://doi.org/10.4271/2024-28-0008

Peng, J., Sun, Z. L., Shi, Y. B., Wang, H. K., Liu, Z. Y., Quan, J. H., Wang, Y. A., Xu, J. P., Zhang, H. R., and Chen, W. X. (2022). "Experimental research on heat transfer performance of single tube multi-row finned tube evaporator," *Journal of Refrigeration* 43(1), 116-122. https://doi.org/10.3969/j.issn.0253-4339.2022.01.116

Qin, Q., Chen, J. S., Tang, K. K., and Chen, X. Q. (2021). "Optimization design of heat transfer oil pipe of asphalt tank based on Fluent," *Construction Machinery* 52(8), 88-92,+11. https://doi.org/10.3969/j.issn.1000-1212.2021.08.018

Spiegel, E. A., and Veronis, G. (1960). "On the Boussinesq approximation for a compressible fluid," *Astrophysical Journal* 131(2), 442-447. https://doi.org/10.1086/146849

Wu, J., Xu, F., Zhang, L., Xi, Y., Liu, Y., Zhang, X., Zhou, C., and Zhao, Y. (2024). "Turbulent flow and heat transfer in a new type of internally torsion-ribbed helical

tube," *Chemical Engineering and Processing - Process Intensification* 200, article 109784. https://doi.org/10.1016/j.cep.2024.109784

Xu, K., Rui, J. N., Zhao, Y. L., Zhang, Z. S., Dong, Z. Q., and Qiu, Y. P. (2025). "Application of water quality purification using bottom ash from direct combustion of agroforestry biomass power plants: properties, effects, mechanisms and prospects," *Journal of Agricultural Resources and Environment* 42(4), 1021-1031. https://doi.org/10.13254/j.jare.2024.0608

Yang, T. (2016). *The Research on the Simulation of the Asphalt Heating Tank Flow Field and the Rationality of Agitator Layout*, Master's Thesis, Taiyuan University of Science and Technology, Taiyuan, China.

Yao, J. C., Liu, J., Wang, J. L., Sun, M. Y., Fang, K., and Shi, B. (2023). "A study of soil thermal conductivity measurement based on the actively heated distributed temperature sensing cable," *Hydrogeology & Engineering Geology* 50(1), 179-188. https://doi.org/10.16030/j.cnki.issn.1000-3665.202111076

Yao, Y. S., Yuan, Y. S., and Zheng, Y. K. (1999). "The effect of the physical properties of thermo oil on its heating system," *Textile Dyeing and Finishing Journal* 21(6), 29-33.

Yu, P. F., Xiao, S., Ge, Z. W., and Yang, T. (2019). "Exergy balance analysis of 10 MW biomass gasification coupled supercritical coal-fired boiler system," *Journal of Engineering for Thermal Energy and Power* 34(12), 131-136. https://doi.org/10.16146/j.cnki.rndlgc.2019.12.019

Zhang, D. W., Shi, J., Yang, H. R., Lyu, J. F., Zhang, M., Huang, Z., and Li, S. Y. (2022). "Prospect of biomass power generation under the background of carbon pricing," *Clean Coal Technology* 28(3), 23-31. https://doi.org/10.13226/j.issn.1006-6772.CC21081601

Article submitted: June 4, 2026; Peer review completed: October 10, 2026; Revised version received: October 19, 2026; Accepted: October 25, 2026; Published: November 6, 2026.
DOI: 10.15376/biores.22.1.42-70